3D reconstruction of a bridge with concrete damage classification using deep learning

Christopher Núñez[a], Marck Regalado [a], Luis Huaypar[a], Antonio Bedón[a], Jordan Romaní[a], Oscar Solís[a], Karol Agreda[a] and Micaela Cárdenas[b]

[a]Faculty of Civil Engineering, National University of Engineering, Perú
[b]Faculty of Civil Engineering, National University of Trujillo, Perú
E-mail: christopher.nunez.v@uni.pe, marck.regalado.e@uni.pe, luis.huaypar.a@uni.pe, antonio.bedon.r@uni.pe, jordan.romani.c@uni.pe, oscar.solis.g@uni.pe, karol.agreda.e@uni.pe and t534000120@unitru.edu.pe

Abstract

The classification of concrete damage in bridges poses challenges, characterized by time-consuming, hazardous, and often subjective inspection methods. Recognizing the need for efficient damage identification and the creation of 3D models for maintenance purposes, this paper introduces an innovative approach to the inspection of reinforced concrete bridges. The proposed methodology involves 3D reconstruction of a bridge, coupled with a concrete damage classification system based on severity. Notably, the analysis ensures objectivity through the implementation of deep learning for classifying concrete damage in UAV-captured images. A noteworthy aspect of this research is that, in the training models, a precision of over 90% is achieved for each type of concrete damage. This methodology serves as a valuable contribution to automating and streamlining concrete bridge inspections, aiming to reduce costs and enhance efficiency throughout its life cycle.

Keywords –

UAV; Bridge; Concrete damage; SHM; CNN

1 Introduction

In contemporary society, bridges hold significant environmental significance by establishing vital connections between various localities. They play a crucial role in fostering economic and cultural development, among other societal factors [1–3]. Therefore, preserving their structural integrity, safety, and functionality is paramount throughout their lifespan, especially for emergency situations such as resource transportation and rescue operations [3,4].

Currently, numerous countries, particularly those in Europe and North America, confront the deterioration of an extensive infrastructure inventory that has surpassed its originally planned service life [1]. In the United States, the report states that 7.5% of bridges are categorized as structurally deficient, predominantly falling below the established standards [5]. In fact, a minimum of one-third of the over 600,000 bridges in the United States feature a concrete superstructure or wearing surface [6].

In recent years, notable bridge collapses attributed to various factors have occurred, including the Morandi cable-stayed bridge in Genoa, Italy (2018), the Florida International University Pedestrian Bridge (2018), and the Nanfang'ao steel single-arch bridge in Taiwan (2019) [4]. Taiwan, with over 28,000 bridges, faces challenges due to natural disasters like earthquakes, typhoons, and rainstorms, along with its unique geographic features, such as mountainous and stream-filled regions. Over the past decades, several bridge collapses have been attributed to various scour issues, including general scour and local scour [3].

Concrete structures are increasingly experiencing deterioration due to various factors such as aging, increased traffic loads, loadings from earthquakes and extreme weather conditions (wind, ambient vibrations) [4,5,7–9], such deterioration is usually caused by inadequate or untimely maintenance [1] Similarly, the prevalent structural configuration employed for bridges has been the multispan design with simply supported Reinforced Concrete (RC) girders. These girders are interconnected by transverse beams and are supported by piers and abutments at the ends, facilitating construction phases [1]. Consequently, while the emergence of cracks in concrete bridges is a crucial indicator of structural performance, it doesn't necessarily signify imminent collapse; however, it frequently results in diminished structural integrity [8,10]. Additionally, concrete damaged impact various aspects of structures, including bearing capacity, stiffness, energy absorption capacity, and resistance to reinforcement corrosion [8,9,11]. Therefore, timely detection and measurement of damaged elements are crucial for making informed decisions regarding necessary repairs and maintenance [8]. However, conventional inspection methods often prove laborious, time-consuming, and capital-intensive. Especially, in the case of large span bridges, traditional methods are not effective for rapid full-field monitoring and hence a radical monitoring approach is most needed [12]. During recent decades, ensuring life safety and the need to reduce inspection costs have emerged as the top priorities for practicing engineers and researchers [5].

Compared to the traditional contact methods, most of the noncontact Structural Health Monitoring (SHM) methods have improvement in the convenience and efficiency of structural inspection and concrete damage [9]. SHM is a data processing approach that employs technology to offer early signals of disruption and the progression of damages and deterioration to avert potentially hazardous results to a specific structure, which is useful for enhanced decision-making [1,7]. The majority of existing SHM system consists of various sensors and accelerometers [7,13,14].

Consequently, an increasingly number of SHM applications with noncontact means have been developed and applied for the monitoring and inspection of concrete damage in a variety of critical concrete structures [9]. The deployment of Unmanned Aerial Vehicles (UAV) for civil infrastructure monitoring is a relatively recent development, with only a limited number of practical case studies conducted for industries, monuments, and other civil structures. Typically, UAVs are equipped with an image acquisition system, and the captured data are manually processed [1,7,12]. While this approach is convenient, it involves labor-intensive efforts in quantifying and analyzing the acquired data [12].

In this paper, we propose a methodology for the classification of damage in the concrete components of a bridge, employing Deep Learning (DL) based method for image processing. DL serves as an automated solution for predicting and classifying data, with the Convolutional Neural Network (CNN) emerging as a prevalent and straightforward method, particularly well-suited for image classification tasks. CNN excels in processing and categorizing information presented in image formats, making it a widely adopted approach in the realm of deep learning [15]. The images utilized in this analysis were captured by an Unmanned Aerial Vehicle (UAV). This approach leverages advanced algorithms to categorize and analyze the identified damaged elements, contributing to a nuanced understanding of structural integrity. The integration of UAV technology and CNN method in the proposed methodology offers a sophisticated and efficient means of assessing the condition of concrete elements in bridge infrastructure. This method extracts features of different abstract levels and maps raw pixel intensities of the crack patch into a feature vector through several fully connected layers. All convolutional filter kernel elements are trained from the data in a supervised fashion, learning from the labeled set of examples. This approach not only leverages advanced aerial imaging capabilities but also employs CNN to automatically extract and analyze features from the captured images, enhancing the precision of structural assessment in the context of concrete damage classification.

The paper is organized as follows: In Section 2, we delve into the Background and Related Studies. Section 3 provides the methodology for obtaining the 3D reconstructed case study with the classification of the damaged concrete using deep learning. The findings of our study are presented in Section 4, which covers the Results. Finally, Section 5 presents the scientific contribution and conclusions of this paper.

2 Background and Related studies

2.1 Concrete Damage classification

During the last three decades, there has been notable expansion in the utilization of high-strength concrete applications in bridge construction [16]. The five most prevalent damage, as outlined in Table 1, encompass cracks, corrosion, efflorescence, spalling, and exposed steel reinforcement [17] . To establish a ranking system for the magnitude of primary damages in reinforced concrete, reference is made to Hüthwohl et al. [18] and Highways England [19] particularly its document "CS 450 Inspection of Highway Structures." This is undertaken with the objective of formulating a model to categorize concrete damages based on their severity.

Hence, we have identified three magnitudes for each concrete damage, serving as benchmarks to evaluate bridge inspection damage classification methods: (1) Not Found (No color), (2) Moderate Damage (Orange color), and (3) Critical Damage (Red color). In instances where multiple damage types coexist, the color corresponding to the highest magnitude will be applied. As such, in the present article, neither the location of the damage nor the combination of types of damage in concrete were taken into consideration when calculating the magnitude. The focus was solely on the damage itself in a 288x288-pixel image. Additionally, due to the variability in image quality, it hinders the analysis of combinations of damage in concrete.

2.2 Relevant studies

The important aspect of the research presented in this paper lies in the utilization of computer vision to identify defects and damages, thereby establishing an objective classification process.

Table 1 Damage scale for reinforced concrete.

Damage	Damage Scale (Color reference)		
	No damage (No color)	Moderate Damage (Orange)	Major Damage (Red)
Corrosion	No signs of corrosion attack	Moderate corrosion attack	Major corrosion attack
Crack	No signs of cracks or difficult to detect visually	Cracks less than 1 mm (difficult to detect visually)	Cracks more than 1 mm (easily visible)
Efflorescence	No signs of efflorescence attack	Moderate efflorescence attack	Major efflorescence attack
Exposed Bars	No exposed bars	Moderately exposed bars	Fully exposed bars
Spallation	No spalls	Minor deep spalls exposing	Collapsed

Mansuri & Patel [20] devised an automated visual inspection system for defect detection in heritage structures, leveraging artificial intelligence through an R-CNN (Faster Region-based Convolutional Neural Network) object detection model. The inspection accuracy of this model demonstrated optimal detection precision, reaching 91.58%, particularly in identifying three damage types: "spalling," "exposed bricks," and "cracks."

Zhao et al. [21] conducted a three-dimensional reconstruction based on images captured by unmanned aerial vehicles for the monitoring and inspection of dams, focusing on the identification of damages in the obtained images. Subsequently, non-contact optical measurements were performed for disaster prevention.

Wang et al. [1] suggested a UAV-based method to promptly evaluate seismic risk in bridges. Their methodology encompassed the acquisition of aerial photogrammetric data and the automated extraction of geometric features, subsequently integrated into structural models to assess seismic risk in relation to capacity-demand. The feasibility of their approach was substantiated through a case study conducted on an Italian bridge, thus contributing valuable insights to the field of seismic risk assessment for infrastructure.

Nappo et al. [22] proposed the utilization of Unmanned Aerial Vehicles (UAVs) for the semi-automatic detection and classification of damages in asphalt-paved roads affected by landslides. Leveraging 3D models and 2D images derived through UAV-based photogrammetry, the approach aimed to overcome the limitations associated with traditional visual inspections. The developed semi-automatic procedure quantitatively identified and classified longitudinal and transverse cracks in the pavement, presenting a swift, systematic, and objective alternative to conventional field surveys. Applied in the Province of Como, Northern Italy, the results underscored the methodology's utility for road management, providing maps of damage hotspots, pavement damage detectors, criteria based on the International Roughness Index (IRI), and road damage severity maps.

3 Methods and Implementations

3.1 Selected UAV

The aerial survey was performed using a commercial quadrotor, Phantom 4 V2. (DJI, China). This portable UAV has a built-in GPS that is used for way-point navigation and dataset geotagging. The drone was deployed for visual inspections of various structural components across four reinforced concrete bridges. Figure 1 illustrates the implementation of the proposed methodology outlined in this paper for bridge inspection utilizing a drone. The specifications of both the vehicle and the camera, outlined in Table 2, play a crucial role in the image processing carried out by the deep learning model.

Table 2 DJI Phantom 4 V2. technical specification.

Unmanned Aerial Vehicle (UAV)		DJI Phantom 4 V2
Dimension (mm)		289.5x289.5x196
Weight (kg)		1.375
Max flight time		Approx. 30 minutes
Hovering flying accuracy (with GPS and vision system)		Vertical: ±0.1m Horizontal: ±0.3m
Max. speed (mph)		45
Photo resolution		5472x3648 pixels
Camera	Sensor	1" CMOS
	Pixels	20 Mega
Remote range (km)		8

Fig. 1. UAV used for the data acquisition

3.2 Data acquisition

The task of data acquisition includes (i) site prechecking of the bridge and surrounding area, (ii) flight plan drafting, and (iii) on-site data collection. Firstly, an examination of the area should be conducted to consider multiple factors such as the complexity of the surroundings and the visibility of the structure (e.g., presence of obstacles/vegetation around the structure), the accessibility of the area to identify suitable take-off and landing points, and flight restrictions according to local regulations (e.g., the presence of no-fly zones, the highest permissible altitude for flying, etc.). Then, the planning of the flight path exerts the most significant influence on data quality, as it pertains to factors such as lighting conditions, camera angles, offset distances, the flight pattern chosen, and the level of overlap between images [1]. Additionally, to explain the relationship between camera angle and distance, the terminology ground sampling distance (GSD) is referred to the ratio between the measure of an actual object to a pixel size [1,23,24], which is used here to describe the image quality.

Our work is motivated by a project aiming at the damage classification in concrete bridge elements within a millimeter (1 mm) of accuracy, which is considered adequate following previous research such as Chen et al. [23] who show a relationship between GSD and Working Distance (WD) for the DJI phantom 4 UAV with respect to the tilt angle and offset distance.

The overlap (OV) represents the percentage of the object covered in two consecutive frames, depending on the distance to the center of two consecutive photos. The value of OV is one of the parameters for determining the fly path in the vertical and horizontal directions. Even though overlapping rates are seldom documented and seem to be chosen based on empirical observations, in Chen et al. [23] it is recommended 60% ±5% for endlap and 30% ±15% for sidelap. In this work, a 60% OV vertical and 30% OV horizontal direction should be considered in the to ensure the survey quality.

After establishing the Ground Sample Distance (GSD), overlap (OV), an appropriate working distance (WD), and tilt angle that align with the research objectives for image acquisition, we then move forward to elucidate the procedure for capturing imagery of the structural elements to create 3D models, as detailed in the subsequent subsection.

3.2.1 Super-structure

Linear trajectories parallel to the longitudinal direction of the bridge and outer beams were employed, adjusting the inclination angle to ensure comprehensive coverage of the structural beam (See Fig. 2).

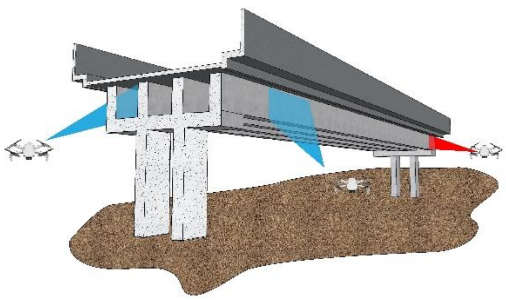

Fig. 2. Image acquisition process of a concrete bridge structural beam.

3.2.2 Sub-structure

In the case of the pillars (see Fig. 3), linear trajectories are executed, aligning with the lateral elevation profile of the bridge at varying heights and employing different camera pitch and yaw angles (including upward orientation for mapping beneath the deck). Where deemed safe, additional spiral (or point of interest) flights along the height of each pillar are conducted to ensure comprehensive coverage of all surfaces. As for the abutments (see Fig. 4), a parallel survey will be conducted along the primary faces, adjusting both the height and inclination angles for a thorough inspection.

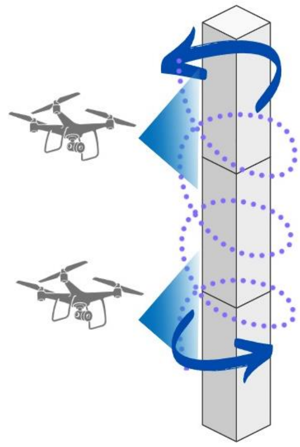

Fig. 3. Image acquisition process of the structural column of a concrete bridge.

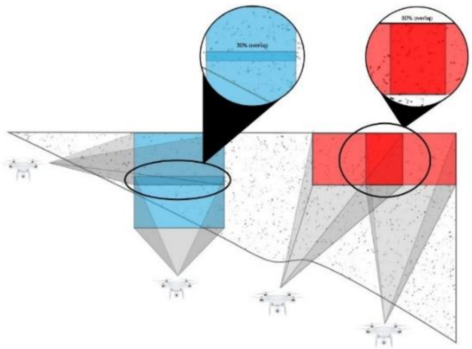

Fig. 4. Image acquisition process of concrete bridge abutments.

3.3 Imagen processing algorithms

The images were captured at a resolution of 5472x3648 pixels from a dataset comprising four distinct bridges. The selection of these bridges was based on a non-probability sampling approach, considering their proximity to the designated study area, The training dataset incorporates images from three of these bridges, totaling 848 images. Additionally, to enhance the performance of our training model, we have incorporated another dataset provided by Hüthwohl et al. [18]. As part of the validation dataset, we have selected the Iniche bridge (refer to Fig. 5) as a case study, yielding a total of 142 images.

Fig. 5 Case study: Iniche bridge. Chiclayo, Perú.

This implies that a higher number of neurons require more parameters to be learned, increasing both the learning time and complexity of the model. To mitigate the size of the CNN model, the original image is resized to a smaller image, specifically 228x228 pixels. Subsequently, 384 images, each measuring 228x228 pixels, were generated for every original image of dimensions 5472x3648 pixels. Regarding the image quality, it is important that the images have a good resolution, such as HD or 4K, since the reduced image used to analyze bridge damage (228 x 228 pixels) may present noise that generates incorrect image treatment in the model. Additionally, the normalization of the pixels should be between 0 and 1, following the image binarization criterion based on Elizondo et al. [25].

3.3.1 Data Preparation

In this paper, we employ a deep convolutional neural network based in Zhang et al., [26]. In the data preparation phase, we implemented a code snippet using the TensorFlow Keras API. This code segment focuses on organizing and structuring the input data for model training. Subsequently, the images are reshaped into the appropriate format for TensorFlow, ensuring compatibility by adjusting the dimensions to (number of images, width, height, channels). The reshaped data is then stored in an HDF5 file format using the h5py library, providing an efficient and compressed representation of the dataset.

3.3.2 Data Training

In the data training phase, we utilized the TensorFlow Keras API to construct a Convolutional Neural Network (CNN) architecture for the classification of concrete damage. The input data, stored in an HDF5 file format, is loaded, and pre-processed, including resizing the images to a standardized dimension of 228x228 pixels and normalizing pixel values between 0 and 1. The CNN model is designed as a sequential stack of layers, starting with a convolutional layer with 16 filters, followed by max-pooling, batch normalization, and dropout for regularization. This pattern is repeated with additional convolutional layers, each increasing the number of filters. The final layer is a dense layer with softmax activation, representing the three categories of damage scale (See Table 1). During training, the model is fed with the pre-processed images, aiming for 30 epochs with a batch size of 64 and a validation split of 20%. The trained model is then saved for subsequent use. This architecture combines convolutional and pooling layers with normalization and dropout techniques, demonstrating its potential for accurate concrete damage classification in structural inspection applications. Regarding the number of images in the training model, this is summarized in the following Table 3. As such, it is important to note that from the set of photos, each image was manually labeled according to the concrete damage.

Table 3 Number of samples used in the training model.

Concrete Damage	Training Samples		
	No damage	Moderate Damage	Major Damage
Corrosion	2180	544	690
Cracks		4609	6998
Efflorescence		1196	1094
Exposed Bars		289	766
Spalling		1310	1592

3.3.3 Data Classification

In this section, a function is developed to manage the loading, resizing, and normalizing each grayscale image to fit the required input dimensions of the model. From the case study, 142 images of 5472x3648 pixels were obtained from which only 89 images were selected for the classification process.

The subsequent iteration through each image file involves making predictions using the loaded model. Additionally, contours are detected in the original image, and based on the predicted class, they are highlighted with semi-transparent colors to emphasize the severity of concrete damage.

Notably, the code incorporates error handling to ensure the successful loading and preparation of images. Furthermore, contours are drawn on images to visually represent the detected damage patterns, contributing to a more comprehensive analysis. The entire process is geared towards automating the classification of concrete damage, making it a valuable tool for efficient structural health assessment.

3.4 3D Reconstruction

The initial step involves the application of colorization to highlight the severity of the damage in each 228x228-pixel image. Subsequently, a meticulous merging process is undertaken to reconstruct these images to their original resolution of 5472x3648 pixels.

This merging process is pivotal, as resizing each image independently would result in the loss of critical georeferencing information. This information, including Latitude, Altitude, Longitude, Focal length, orientation, and other metadata, is embedded in the data provided by the drone for each image. Maintaining the integrity of this georeferencing data is essential for the accuracy of the final 3D spatial reconstruction.

Following the image merging, each reconstructed image is meticulously reassigned its corresponding metadata. This involves a comprehensive analysis and adjustment to ensure that the geospatial information aligns accurately with the reconstructed visual data.

To achieve a technically robust 3D reconstruction, specialized software designed for photogrammetric processing of digital images is employed. Notably, Agisoft Metashape stands out as a prominent example of such software. This software employs advanced algorithms and techniques to process the merged images and generate precise 3D spatial data.

4 Results

4.1 Data Training

The key metrics during the training of the deep learning model are summarized in Table 4.

Table 4. Loss and accuracy of the training model

Concrete Damage	Epoch	Training Loss (Accuracy)	Validation Loss (Accuracy)
Corrosion	1/30	1.0573 (0.7799)	4.4956 (0.6442)
	30/30	0.0928 (0.9766)	3.3723 (0.5447)
Cracks	1/30	1.0725 (0.7264)	9.1893 (0.1653)
	30/30	0.1149 (0.9625)	0.6825 (0.8677)
Efflorescence	1/30	1.5263 (0.6063)	1.0956 (0.3747)
	30/30	0.1526 (0.9452)	2.6873 (0.6756)
Exposed Bars	1/30	0.9333 (0.8396)	2.0844 (0.6909)
	30/30	0.0388 (0.9884)	1.1794 (0.8779)
Spalling	1/30	1.4644 (0.6148)	1.9797 (0.4435)
	30/30	0.1393 (0.9542)	2.9182 (0.5280)

4.2 Data Classification

Given the extensive dataset, we present a table displaying the classification of select images featuring damaged concrete along with their corresponding confidence levels.

In Table 5, the classification results of concrete damage for a photograph are illustrated. It can be observed that, in the case of the example, after processing, only corrosion, efflorescence, and spalling damage are noticeable. Similar results are obtained for all other photographs based on the level of damage they exhibit.

4.3 3D Reconstruction

After the classification process, the 228x228 pixels colored images are combined with their counterparts from the original image, which is 5472x3648 pixels (See Fig. 6). Subsequently, the metadata from the original image is transferred to the reconstructed image.

Table 5. Classification results for concrete damage in a 288x288 pixel example photograph

Concrete Damage	Example image	Damage Classification (Level of confidence)
Corrosion		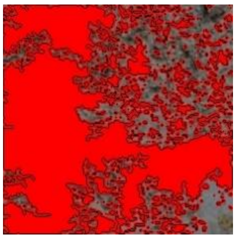 Major (59.74%)
Cracks		 No color (100.00%)
Efflorescence	 (228x228 pixels)	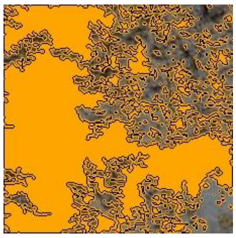 Moderate (98.06%)
Exposed Bars		 No color (88.44%)
Spalling		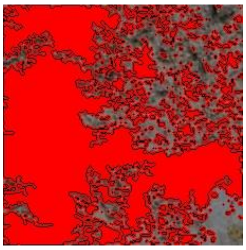 Major (99.88%)

Fig. 6 Reconstructed image with concrete damage classification

Ultimately, utilizing these 89 reconstructed images from the case study, we proceed to generate a point cloud and perform the 3D reconstruction of the bridge (See Fig. 7).

Fig. 7 3D reconstruction of the Iniche bridge with concrete damage classification

5 Conclusions and discussions

The proposed methodology demonstrates efficiency in bridge inspections by combining three-dimensional reconstruction with concrete damage classification using deep learning. This suggests an effective and automated alternative for assessing bridge conditions, minimizing time and costs associated with traditional methods.

The implementation of deep learning in concrete damage classification ensures an objective approach. The model's ability to accurately identify and categorize defects in concrete from UAV-captured images suggests a significant improvement in result objectivity compared to conventional inspection methods.

Upon reviewing the outcomes derived from the 228x228 pixel images, it is evident that a more extensive dataset is essential for refining the training model. Also, due to the use of an external database, the GDS has been variable which affects the quality of the images and therefore affects the training database.

Addressing the loss of georeferenced information after resizing images is achieved through three-dimensional reconstruction, where the original metadata is transferred to the reconstructed images. This highlights the importance of integrating geospatial data for a more comprehensive and accurate assessment of infrastructure.

The main limitations of this method were that it does not assess the quality of the images due to their reduction in size. Additionally, the classification of the magnitude of the damage was partially subjective. Other limitations included the acquisition of data, where external conditions to the infrastructure, such as the flow of a river, varied the quality of the images.

References

[1] Wang X, Demartino C, Narazaki Y, Monti G, Spencer BF. Rapid seismic risk assessment of bridges using UAV aerial photogrammetry. Eng Struct. 2023 Mar 15;279:115589.

[2] Scattarreggia N, Salomone R, Moratti M, Malomo D, Pinho R, Calvi GM. Collapse analysis of the multi-span reinforced concrete arch bridge of Caprigliola, Italy. Eng Struct. 2022 Jan 15;251:113375.

[3] Yau NJ, Tsai MK, Wang HL, Hung DM, Chen CS, Hsu WK. Improving bridge collapse detection and on-site emergency alarms: A case study in Taiwan. Saf Sci. 2014 Dec 1;70:133–42.

[4] Mandirola M, Casarotti C, Peloso S, Lanese I, Brunesi E, Senaldi I. Use of UAS for damage inspection and assessment of bridge infrastructures. International Journal of Disaster Risk Reduction. 2022 Apr 1;72:102824.

[5] Azimi M, Eslamlou AD, Pekcan G. Data-Driven Structural Health Monitoring and Damage Detection through Deep Learning: State-of-the-Art Review. Sensors [Internet]. 2020;20(10). Available from: https://www.mdpi.com/1424-8220/20/10/2778

[6] Dorafshan S, Thomas RJ, Maguire M. Comparison of deep convolutional neural networks and edge detectors for image-based crack detection in concrete. Constr Build Mater. 2018 Oct 20;186:1031–45.

[7] Payawal JMG, Kim DK. Image-Based Structural Health Monitoring: A Systematic Review. Applied Sciences [Internet]. 2023;13(2). Available from: https://www.mdpi.com/2076-3417/13/2/968

[8] Nyathi MA, Bai J, Wilson ID. Concrete Crack Width Measurement Using a Laser Beam and Image Processing Algorithms. Applied Sciences [Internet]. 2023;13(8). Available from: https://www.mdpi.com/2076-3417/13/8/4981

[9] Zhang Z, Zhou H, Wang S, Xu C, Lv Y. Design and Research of Low-Cost and Self-Adaptive Terrestrial Laser Scanning for Indoor Measurement Based on Adaptive Indoor Measurement Scanning Strategy and Structural

Characteristics Point Cloud Segmentation. Han J, editor. Advances in Civil Engineering [Internet]. 2022;2022:5681771. Available from: https://doi.org/10.1155/2022/5681771

[10] Zoubir H, Rguig M, El Aroussi M, Chehri A, Saadane R. Concrete Bridge Crack Image Classification Using Histograms of Oriented Gradients, Uniform Local Binary Patterns, and Kernel Principal Component Analysis. Electronics (Basel) [Internet]. 2022;11(20). Available from: https://www.mdpi.com/2079-9292/11/20/3357

[11] Li J, Li X, Liu K, Yao Z. Crack Identification for Bridge Structures Using an Unmanned Aerial Vehicle (UAV) Incorporating Image Geometric Correction. Buildings [Internet]. 2022;12(11). Available from: https://www.mdpi.com/2075-5309/12/11/1869

[12] Sankarasrinivasan S, Balasubramanian E, Karthik K, Chandrasekar U, Gupta R. Health Monitoring of Civil Structures with Integrated UAV and Image Processing System. Procedia Comput Sci. 2015 Jan 1;54:508–15.

[13] Bao Y, Chen Z, Wei S, Xu Y, Tang Z, Li H. The State of the Art of Data Science and Engineering in Structural Health Monitoring. Engineering. 2019 Apr 1;5(2):234–42.

[14] Ye XW, Dong CZ, Liu T. A Review of Machine Vision-Based Structural Health Monitoring: Methodologies and Applications. Oddo CM, editor. J Sens [Internet]. 2016;2016:7103039. Available from: ttps://doi.org/10.1155/2016/7103039

[15] Permana SDH, Saputra G, Arifitama B, Yaddarabullah, Caesarendra W, Rahim R. Classification of bird sounds as an early warning method of forest fires using Convolutional Neural Network (CNN) algorithm. Journal of King Saud University - Computer and Information Sciences. 2022 Jul 1;34(7):4345–57.

[16] Sagara A, Pane I. A Study on Effects of Creep and Shrinkage in High Strength Concrete Bridges. Procedia Eng. 2015 Jan 1;125:1087–93.

[17] Abubakr M, Rady M, Badran K, Mahfouz SY. Application of deep learning in damage classification of reinforced concrete bridges. Ain Shams Engineering Journal. 2024 Jan 1;15(1):102297.

[18] Hüthwohl P, Lu R, Brilakis I. Multi-classifier for reinforced concrete bridge defects. Autom Constr. 2019 Sep 1;105:102824.

[19] Highways England. CS 450 Inspection of highway structures. In: 0.1.0. Design Manual for Roads and Bridges; 2021.

[20] Mansuri L, Patel D. Artificial intelligence-based automatic visual inspection system for built heritage. Smart and Sustainable Built Environment. 2021 Feb 3;11:622–46.

[21] Zhao S, Kang F, Li J, Ma C. Structural health monitoring and inspection of dams based on UAV photogrammetry with image 3D reconstruction. Autom Constr. 2021 Oct 1;130:103832.

[22] Nappo N, Mavrouli O, Nex F, van Westen C, Gambillara R, Michetti AM. Use of UAV-based photogrammetry products for semi-automatic detection and classification of asphalt road damage in landslide-affected areas. Eng Geol. 2021 Dec 5;294:106363.

[23] Siyuan C, F LD, Eleni M, Iman ZSM, Jonathan B. UAV Bridge Inspection through Evaluated 3D Reconstructions. Journal of Bridge Engineering [Internet]. 2019 Apr 1;24(4):05019001. Available from: https://doi.org/10.1061/(ASCE)BE.1943-5592.0001343

[24] Atencio E, Plaza-Muñoz F, Muñoz-La Rivera F, Lozano-Galant JA. Calibration of UAV flight parameters for pavement pothole detection using orthogonal arrays. Autom Constr. 2022 Nov 1;143:104545.

[25] Esqueda Elizondo J, Palafox L. Fundamentos de Procesamiento de Imágenes. 2005.

[26] Zhang L, Yang F, Daniel Zhang Y, Zhu YJ. Road crack detection using deep convolutional neural network. In: 2016 IEEE International Conference on Image Processing (ICIP). 2016. p. 3708–12.